Quantum phases of a dipolar Bose-Einstein condensate in an optical lattice with three-body interaction

Kezhao Zhou (周可召), Zhaoxin Liang (梁兆新),* and Zhidong Zhang (张志东)
Shenyang National Laboratory for Materials Science, Institute of Metal Research, and International Centre for Materials Physics, Chinese Academy of Sciences, 72 Wenhua Road, Shenyang 110016, People's Republic of China
(Received 29 March 2010; published 26 July 2010)

We investigate the quantum phases of a dipolar Bose-Einstein condensate (BEC) in an optical lattice based on the extended Bose-Hubbard model taking into account the three-body scattering. Accordingly, the phase diagrams from the superfluid state to the Mott-insulator state for such BEC systems are obtained and analyzed, employing both the mean-field approach and the functional-integral method. In particular, we explore the combined effects of three-body interaction and dipole-dipole interaction on the insulating *lobes* in detail. The experimental scenario is also discussed.

DOI: 10.1103/PhysRevA.82.013634 PACS number(s): 03.75.Hh, 05.30.Jp, 03.75.Lm

I. INTRODUCTION

The effects of dipole-dipole interactions on the quantum phases of a Bose-Einstein condensate (BEC) in an optical lattice have attracted huge interest recently for at least three reasons [1]. First, the possibility of engineering lattice models almost at will provides one of the most promising routes in searching for exotic quantum phases which escape clean demonstration in condensed-matter systems [2–5]. Second, significant experimental progress has been made in recent years in the cooling and trapping of polar molecules and of atomic species that have a large magnetic moment [6–9]. These amazing experimental achievements have therefore opened new windows in investigating degenerate gases with dominant dipole-dipole interactions. Finally, due to the long-range and anisotropic properties that characterize dipolar interactions, the physics of a BEC system is significantly enriched [1,10]. In particular, dipolar forces have been shown to considerably modify the ground-state and collective excitations of trapped condensates [11–13], whereas the interplay of short-range scattering and long-range interaction may give rise to such phenomena as ferromagnetic order, spin waves, and other exotic phases [14–16]. Moreover, since dipole-dipole interactions can be quite strong relative to the short-range (contact) interactions, dipolar particles are considered to be promising candidates for the implementation of fast and robust quantum-computing schemes [1,17,18].

Along this line, intensive theoretical investigations have been carried out so far on the BEC system trapped in an optical lattice that has dipole-dipole interaction [1]. To our best knowledge, however, these investigations have ignored the interaction among three or more bosonic atoms. In particular, most previous investigations were based on an extended Bose-Hubbard model (BHM) that highlights the competition between the kinetic energy, which is gained by delocalizing particles over lattice sites, and the combined repulsive on-site interaction and the dipole-dipole interaction, which disfavors having more than one particle at a given site. Hence, an important question immediately arises on the unique role played by three-body interaction in the BHM for a dipolar BEC.

In particular, the three-body interaction arising from triple collisions can be obtained by studying the three-body scattering problem and is characterized by the three-body coupling constant within the context of pseudopotentials. The theoretical determination of the three-body coupling constant in a dilute BEC has a long history of research, dating back to 1959 when Wu [19] predicted a general form, that is, $g_3 = 16\pi\hbar^2 a_s^4(4\pi - 3\sqrt{3})\ln(C\sqrt{na_s^3})/m$, for a Bose gas of hard spheres. Here, the constant C was only determined recently by Braaten and Nieto [20] using effective field theory. This general expression for g_3 was confirmed by Köhler in a recent paper [21] which derived the explicit three-body contact potential for a dilute Bose gas from microscopic theory. On the other hand, there have also been efforts in identifying experimentally accessible systems that have three-body or higher interactions. In particular, Büchler *et al.* [22] reported that polar molecules interacting via dipolar interactions driven by microwave fields can manifest themselves as a BHM with two- and three-body interaction between nearest neighbors. For on-site interactions, however, Johnson [23] has shown that the two-body collisions of atoms confined in the lowest vibrational states of a three-dimensional optical lattice can generate effective three-body and higher interactions.

In this paper, we launch a systematic investigation on a dipolar BEC in an optical lattice based on an extended BHM taking into account the three-body scattering. In particular, we explore the quantum phases of such BEC systems by employing a mean-field approach to the BHM and, accordingly, we obtain phase boundaries between the superfluid and the Mott-insulator phase. A detailed analysis for the combined effects of three-body interaction and dipole-dipole interaction on the insulating *lobes* is presented, using the functional-integral method. Finally, the experimental scenario is also discussed.

The paper is organized as follows. In Sec. II, we introduce the effective Hamiltonian for a dipolar BEC in an optical lattice with the three-body repulsive interaction within the context of an extended BHM. In Sec. III, we present a mean-field treatment of this extended BHM suitable for describing the Mott-insulating phase transition. In particular, we calculate the ground-state energy correct up to the fourth order of the superfluid order parameter. We also derive the equation for the phase boundary separating the Mott-insulator and

*zhxliang@gmail.com

superfluid regime, using the Landau order parameter expansion for second-order phase transitions. In Sec. IV, we investigate the quantum fluctuations in the Mott-insulating phase using a path-integral method with the help of the Hubbbard-Stratonovich transformation. Accordingly, we derive the excitation spectrum of quasiparticles and quasiholes. Finally, in Sec. V, we summarize our results and propose experimental conditions for realizing our scenario.

II. EXTENDED BOSE-HUBBARD MODEL

In this paper, we discuss the situation where the laser intensity is sufficiently large and the chemical potential μ is small compared to the interband gap. We thereby confine ourselves to the lowest Bloch band. The behavior of such BEC systems can be described within the context of the BHM, extended to account for the presence of dipole-dipole and three-body interactions. The Hamiltonian of the extended BHM using the single-band approximation is [1]

$$H = -t\sum_{\langle i,j\rangle} b_i^\dagger b_j - \mu\sum_i n_i + \frac{U_0}{2}\sum_i n_i(n_i-1) + \frac{W}{6}\sum_i n_i(n_i-1)(n_i-2) + \sum_{\vec{l}}\sum_{\langle\langle i,j\rangle\rangle_{\vec{l}}} \frac{U_{\vec{l}}}{2} n_i n_j. \quad (1)$$

Here, the operators $b_i^\dagger$ (b_i) are the creation (annihilation) particle operators relative to a particle at the lattice site i that is in a state described by the Wannier function $w(\mathbf{r}-\mathbf{r}_i)$ of the lowest energy band, localized on this site. The corresponding particle number operator is $n_i = b_i^\dagger b_i$. The chemical potential μ is introduced to conserve the total number of atoms in the grand-canonical ensemble. The notation $\langle i,j\rangle$ represents nearest neighbors, whereas $\langle\langle i,j\rangle\rangle_{\vec{l}}$ represents neighbors with a relative displacement $\vec{l}$. Hamiltonian (1) is characterized by four parameters: the tunneling rate t, the on-site s-wave scattering interaction U_0, the three-body interaction W arising from triple collisions, and the dipole-dipole interaction at different relative distances $U_{\vec{l}}$.

The tunneling parameter t in Eq. (1) can be calculated from

$$t = \int w^*(\mathbf{r}-\mathbf{r}_i)\left(-\frac{\hbar^2}{2m}\nabla^2 + V_{\text{opt}}(\mathbf{r})\right) w(\mathbf{r}-\mathbf{r}_j)\, d\mathbf{r}, \quad (2)$$

where i and j are indices of the neighboring sites, and $V_{\text{opt}}(\mathbf{r})$ is a three-dimensional external optical potential in the form

$$V_{\text{opt}}(\mathbf{r}) = sE_R[\sin^2(q_B x) + \sin^2(q_B y) + \sin^2(q_B z)]. \quad (3)$$

Here, s is a dimensionless factor labeled by the intensity of the laser beam, and $E_R = \hbar^2 q_B^2/2m$ is the recoil energy with $\hbar q_B$ being the Bragg momentum and m being the mass of an atom. The lattice period is fixed by π/q_B.

The on-site two-body interaction in Eq. (1) is characterized by U_0, which can be calculated as

$$U_0 = \frac{4\pi\hbar^2 a_s}{m}\int d\mathbf{r}|w(\mathbf{r})|^4, \quad (4)$$

where a_s is the s-wave scattering length.

The three-body interaction arising from triple collisions in Eq. (1) is characterized by the parameter W given by [19,24]

$$W = \frac{16\pi\hbar^2}{m} a_s^4 \ln(C\eta^2)\int |w(\mathbf{r})|^6 d\mathbf{r}, \quad (5)$$

where $\eta = \sqrt{|\psi|^2 a_s^3}$ is the dilute gas parameter and the constant C was given in Ref. [21]. We point out that the three-body scattering is treated here as a perturbation to the usual two-body pseudopotential. In case of strong on-site three-body interactions, one has to account for the loss of three-body recombination. In this case, the coupling constant W acquires an imaginary part which corresponds to the threshold formation of dimer molecules and is related to the three-body recombination rate constant K_3 for a Bose gas through $2ImW/\hbar = -K_3/6$ [21]. In the presence of bound states, the condensate can assume only a metastable state. The change of its density, however, is negligible on time scales comparable to collisional durations, so the present result of Eq. (5) remains valid. For example, using the three-body loss rate $\simeq 6\times10^{-30}\ \text{cm}^6\ \text{s}^{-1}$, the loss rate for n atoms in a 40-kHz lattice is $2.5n^2\ \text{s}^{-1}$ and the lifetime for $n=3$ atoms is $\geqslant 60$ ms [23]. The case involving strong three-body interaction is out of the scope of this paper, and we confine ourselves to the parameter regime where Eq. (5) remains valid. We also want to point out that when a three-body bound state emerges close to the zero-energy threshold, the real part of W can assume all positive and negative values in complete analogy to the two-body case. This phenomenon has been connected with the formation of an Efimov state [25] in the three-body energy spectrum in Ref. [26]. In this work, we focus on the superfluid–Mott-insulator phase transition where both two- and three-body interactions are far away from the resonant point. Under this assumption, we can ignore the possibility of forming an Efimov state.

In the tight-binding limit, $\overline{W}$ can be related to $\overline{U}_0$ through [24]

$$\overline{W} = (3\pi)^{-3/2}\ln(C\eta^2)\left(\frac{V_0}{E_R}\right)^{3/4} e^{-2\sqrt{\frac{V_0}{E_R}}} a_s^2 k_L^2 \overline{U}_0^2, \quad (6)$$

where a scaling with respect to zt has been applied so that both $\overline{W}$ and $\overline{U}_0$ are dimensionless. Usually, the experimental value of $a_s^2 k_L^2$ varies from 10^{-10} to 10^{-2} [27]. Within this range, the effect of three-body interactions is very small compared to two-body interactions according to Eq. (6) and is therefore difficult to observe in experiments. However, as pointed out in Ref. [22], by loading the polar molecules into an optical lattice and adding an external microwave field, one can achieve a situation where only observable three-body interaction exists. Hence, it is necessary to investigate the unique role played by three-body interactions in the BHM.

The dipole-dipole interaction, represented by the last term in Eq. (1), is long range and anisotropic in nature, which brings new features to the BHM. In particular, the contribution of dipole-dipole interaction to the BHM can be decomposed into an on-site component and a long-range component. The on-site dipole-dipole interaction U_d is given by [28]

$$U_d = \frac{1}{2\pi}\int d\mathbf{q}\tilde{V}(q)\tilde{n}^2(q), \quad (7)$$

where $\tilde{V}(q)$ and $\tilde{n}(q)$ are the Fourier transform of the dipole potential and density, respectively [12]. On the other hand, within the context of the tight-binding approximation, the long-range part of the dipole-dipole interaction $U_{\vec{l}}$ can be well represented by the interaction between two dipoles localized at sites i and j, respectively:

$$U_{\vec{l}} = D^2[1 - 3\cos^2(\alpha_{\vec{l}})]/l^3 n_i n_j, \tag{8}$$

where D is the dipole moment, and l and $\alpha_{\vec{l}}$ represent the distance and orientation angle, respectively, between the two dipoles. In particular, the main contribution to Eq. (7) arises from dipoles in the nearest vicinity of each other; that is, $U_{\rm NN} = D^2[1 - 3\cos^2(\alpha_{\vec{l}})]/l^3 n_i n_{i\pm1}$.

The total on-site interaction U includes contributions from both two-body and dipole-dipole interaction [28]: $U = U_0 + U_d$. The ratio between U and the nearest-neighbor dipole-dipole interaction $U_{\rm NN}$ characterizes the competition between a short-range interaction and a long-range interaction. In this work, we focus on the limit $U \gg U_{\rm NN}$, where the long-range part of the dipole-dipole interaction can be ignored. In this limit, the Hamiltonian (1) can be approximated as

$$\begin{aligned} H = &-t\sum_{\langle i,j\rangle} b_i^\dagger b_j - \mu\sum_i n_i + \frac{U_0}{2}\sum_i n_i(n_i - 1) \\ &+ \sum_i \frac{U_d}{2} n_i n_i + \frac{W}{6}\sum_i n_i(n_i - 1)(n_i - 2). \end{aligned} \tag{9}$$

In practice, the ratio $U/U_{\rm NN}$ is usually adjusted by tuning the on-site dipole-dipole interaction U_d from negative to positive, either through changing the vertical confinement or through changing the s-wave scattering length via a Feshbach resonance [29]. An alternative approach was recently proposed, using particles that possess large dipole moments such as heteronuclear molecules and Rydberg atoms [1].

III. GROUND-STATE ENERGY AND PHASE DIAGRAM

In this section, we investigate the ground-state energy and the phase diagram for the extended BHM (9) within the context of mean-field approximation [30], in the limit $U \gg U_{\rm NN}$.

A. Ground-state energy

In analogy with Bogoliubov's theory, the mean-field approach to Eq. (1) consists of introducing a superfluid order parameter defined by

$$\psi = \langle b_i^\dagger\rangle = \langle b_i\rangle = \sqrt{n_0}, \tag{10}$$

where n_0 is the condensate fraction at site i. Through introducing a new set of operators $c_i = b_i - \psi$ and $c_i^\dagger = b_i^\dagger - \psi$, one can cast Eq. (9) into an effective Hamiltonian that is correct up to second order in ψ:

$$H^{\rm eff} = H^{(0)} - \psi(c^\dagger + c) + |\psi|^2, \tag{11}$$

where

$$\begin{aligned} H^{(0)} = &(\overline{U}_0/2)n(n-1) - \overline{\mu}n + (z\overline{U}_d/2)n^2 \\ &+ (\overline{W}/6)n(n-1)(n-2) \end{aligned} \tag{12}$$

is the dimensionless expression for the zero-order effective Hamiltonian with $\overline{U}_0$, $\overline{\mu}$, $\overline{U}_d$, and $\overline{W}$ being dimensionless quantities after scaling the corresponding counterparts with zt. Also note that we have dropped the subscript i in Eqs. (11) and H^0 because $H_i^{\rm eff}$ is site independent.

The $H^{(0)}$ in Eq. (12) can be diagonalized in Fock space. The resulting dimensionless zero-order ground-state energy is given by

$$\begin{aligned} E_g^{(0)} &= \min\{E_n^{(0)} | n = 0,1,2,\ldots\} \\ &= \frac{\overline{U}_0}{2}g(g-1) - \overline{\mu}g + \frac{z\overline{U}_d}{2}g^2 + \frac{\overline{W}}{6}g(g-1)(g-2), \end{aligned} \tag{13}$$

where $E_n^{(0)} = \frac{\overline{U}_0}{2}n(n-1) - \overline{\mu}n + \frac{z\overline{U}_d}{2}n^2 + \frac{\overline{W}}{6}n(n-1)(n-2)$ is the eigenvalue of $H^{(0)}$ associated with eigenstate $|n\rangle$, of which the state with $n = g$ particles is the ground state.

After $E_g^{(0)}$ is obtained, we can then treat the last two terms in Eq. (11) as a small perturbation. Following Ref. [31], we find that the correction to $E_g^{(0)}$ in arbitrary order of ψ is given by

$$E_g^{(n)} = {\rm Tr}\left(\sum_{\{n-1\}} S_g^{k_0}\hat{V}\cdots\hat{V}S_g^{k_n}\right), \tag{14}$$

where $\{n\} = \{k_0,\ldots,k_n | k_0 + \cdots + k_n = n|\}$ and

$$S_g^k = \begin{cases} -|g\rangle\langle g| & \text{if } k = 0, \\ \sum_{n\neq g}\frac{|n\rangle\langle n|}{\left(E_g^{(0)} - E_n^{(0)}\right)^k} & \text{if } k > 0. \end{cases} \tag{15}$$

Because of $\hat{V} \sim (c^\dagger + c)$, it follows from Eqs. (14) and (15) that the energy corrections vanish for all odd order n.

Consequently, by summing Eqs. (13) and (14), one obtains the dimensionless total ground-state energy E_g correct up to the quadratic order in ψ as

$$E_g(\psi) = a_0 + a_2|\psi|^2 + a_4|\psi|^4 + 0(|\psi|^6), \tag{16}$$

with

$$a_2 = \frac{g}{F(g) - \overline{\mu}} - \frac{g+1}{F(g+1) - \overline{\mu}} + 1 \tag{17}$$

and

$$\begin{aligned} a_4 = &-\frac{(g+1)(g+2)}{[F(g+1) - \overline{\mu}]^2 H(g+2)} + \frac{g(g-1)}{[F(g) - \overline{\mu}]^2 H(g)} \\ &- \left(\frac{g}{F(g) - \overline{\mu}} - \frac{g+1}{F(g+1) - \overline{\mu}}\right) \\ &\times \left(\frac{g+1}{[F(g+1) - \overline{\mu}]^2} + \frac{g}{[F(g) - \overline{\mu}]^2}\right). \end{aligned} \tag{18}$$

In Eqs. (17) and (18), functions $F(g)$ and $H(g)$ are respectively defined as

$$F(g) = \overline{U}_0(g-1) + \frac{z\overline{U}_d}{2}(2g-1) + \frac{\overline{W}}{2}(g-1)(g-2) \tag{19}$$

and

$$H(g) = (2g-3)\overline{U}_0 + 2(g-1)z\overline{U}_d + (g-2)^2\overline{W} - 2\overline{\mu}. \tag{20}$$

B. Phase diagram

We now investigate the quantum phases of the extended BHM. In particular, we derive the equation for the phase boundary between the superfluid regime and the Mott-insulating regime, using the Landau order parameter expansion for second-order phase transitions.

By minimizing the ground-state energy functional $E_g(\psi)$ in Eq. (16) with respect to ψ, one finds $|\psi|^2 = -a_2/a_4$. Thus, by setting $a_2 = 0$ in Eq. (17), we obtain the equation for the phase boundary between the superfluid and the insulator regime in the phase diagram,

$$\overline{\mu}_{\pm} = \frac{F(g) + F(g+1) - 1 \pm \sqrt{\Delta}}{2}, \tag{21}$$

where

$$\Delta = [F(g+1) - F(g) - (2g+1)]^2 - 4g(g+1). \tag{22}$$

The subscript $\pm$ in Eq. (21) refers to the upper and lower halves of the Mott-insulating region of the phase space. Since $\overline{\mu}_{\pm}$ must be real, Eq. (21) must satisfy the condition $\Delta \geqslant 0$, thereby providing a lower bound to the parameter space; that is,

$$\overline{U}_0 + z\overline{U}_d + (g-1)\overline{W} \geqslant (2g+1) + \sqrt{4g(g+1)}. \tag{23}$$

To investigate the quantum phases as a consequence of the combined effects of the on-site s-wave interaction U_0, the on-site dipole-dipole interaction U_d, and the three-body interaction W, we take the following two consecutive steps.

In the first step, we fix one of the three parameters (U_0, U_d, W) while varying the other two. The results are shown in Fig. 1. In Fig. 1(a), for example, we plot a three-dimensional (3D) phase diagram by varying U_0 and W while keeping U_d fixed. The diagram shows that the increase in dipole-dipole interaction not only fattens the insulating lobes but also shifts them upward.

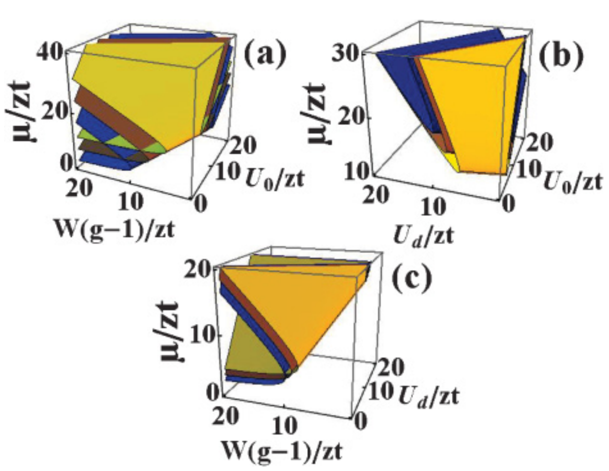

FIG. 1. (Color online) Three-dimensional phase diagram of the extended BHM for $g = 2$ obtained from second-order perturbation theory. The areas enclosed within lobes indicate the insulating phase. Space outside these curved surfaces represents the superfluid phase. The parameters are given as follows: (a) the blue (brown, yellow) surfaces correspond to $U_d/zt = 0$ (0.5,1), (b) the blue (brown, yellow) surfaces correspond to $W/zt = 0$ (2,4), and (c) the blue (brown, yellow) surfaces correspond to $U_0/zt = 0$ (1,2).

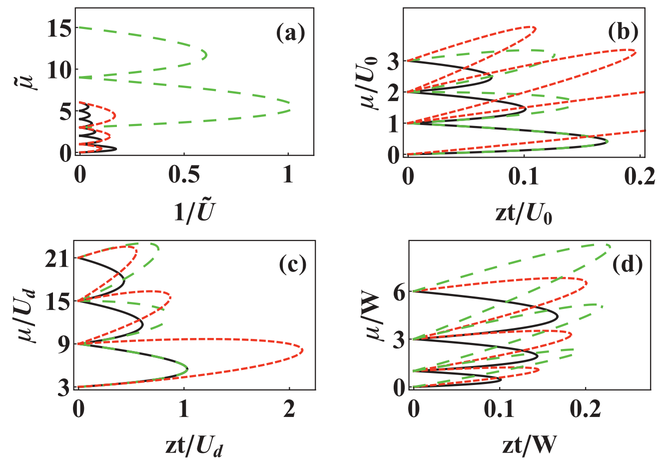

FIG. 2. (Color online) Two-dimensional phase diagram of the extended BHM: plots of Eq. (21) as functions of one of the three interaction parameters with the remaining two fixed. (a) Black curve, $\widetilde{\mu} = \mu/U_0$ and $\widetilde{U} = U_0/zt$ with $g = 1$–6 and $W = U_d = 0$; long-dashed (green) curve, $\widetilde{\mu} = \mu/U_d$ and $\widetilde{U} = U_d/zt$ with $g = 1$–3 and $W = U_0 = 0$; (red) dashed curve, $\widetilde{\mu} = \mu/W$ and $\widetilde{U} = W/zt$ with $U_0 = U_d = 0$. (b) For $g = 1$–3, black curve, $W = U_d = 0$; (red) dashed curve, $W = 0$ and $U_d/zt = 0.8$; and (green) long-dashed curve, $W/zt = 3$ and $U_d = 0$. (c) For $g = 1$–3, black curve, $W = U_0 = 0$; (red) dashed curve, $W = 0$ and $U_0/zt = 3$; and (green) long-dashed curve, $W/zt = 3$ and $U_0 = 0$. (d) For $g = 2$–4, black curve, $U_0 = U_d = 0$; (red) dashed curve, $U_d = 0$ and $U_0/zt = 3$; and (green) long-dashed curve, $U_d/zt = 0.8$ and $U_0 = 0$.

In the second step, we fix two of the three parameters and plot the phase diagram with respect to the remaining one, as shown in Fig. 2. Figure 2(a) shows the superfluid phase and Mott-insulator lobes of the condensate having pure two-body interaction, three-body interaction, and dipole-dipole interaction, respectively. As shown in Fig. 2(a), both three-body and dipole-dipole interactions considerably enlarge the areas of Mott lobes. The Mott lobes for a BEC with pure two-body and dipole-dipole interactions shrink with increasing g as can been seen in Fig. 2(a), whereas Mott lobes induced by three-body interaction enlarge with increasing g. In addition, the breadth of different U_0 lobes is 1, while the breadth of W and U_d lobes is expanding according to $(g-1)$ and z, respectively. Moreover, one can obtain the critical values for the on-site interaction $U_0 + U_d$ and three-body interaction W for each lobe from Eq. (23). By equating the left- and right-hand sides, one finds $\overline{U}_c + (g-1)\overline{W}_c = 2g + 1 + 2\sqrt{g(g+1)}$, where U_c and W_c denote the critical values of $U_0 + U_d$ and W, respectively. In particular, the result $\overline{U}_c \simeq 5.83$ for $g = 1$ is consistent with the corresponding one in Ref. [30].

IV. QUANTUM FLUCTUATIONS IN THE MOTT-INSULATING PHASE: A PATH-INTEGRAL APPROACH

In this section, we investigate the quantum fluctuations in the Mott-insulating (MI) phase arising from the hopping of atoms between sites which causes variations in the site occupancy. Such fluctuations can be described as quasiparticle and quasihole excitations. In what follows, we derive the quasiparticle and quasihole dispersions using the functional-integral method [30,32].

Our starting point is the grand-canonical partition function

$$Z = \int D[\bar{\varphi},\varphi] e^{-\frac{1}{\hbar} S[\bar{\varphi},\varphi]}, \tag{24}$$

where the action $S[\bar{\varphi},\varphi]$ corresponding to Hamiltonian (9) is given by

$$\begin{aligned} S[\bar{\varphi},\varphi] = \int_0^{\hbar\beta} d\tau \Bigg[&\sum_i \bar{\varphi}_i \left(\hbar \frac{\partial}{\partial_\tau} - \mu\right) \varphi_i - \sum_{\langle i,j\rangle} t_{ij} \bar{\varphi}_i \varphi_j \\ &+ \frac{U_0}{2} \sum_i \bar{\varphi}_i \bar{\varphi}_i \varphi_i \varphi_i + \frac{U_d}{2} \sum_{\langle i,j\rangle} \bar{\varphi}_i \bar{\varphi}_j \varphi_j \varphi_i \\ &+ \frac{W}{6} \sum_i \bar{\varphi}_i \bar{\varphi}_i \bar{\varphi}_i \varphi_i \varphi_i \varphi_i \Bigg]. \end{aligned} \tag{25}$$

In Eqs. (24) and (25), $[\bar{\varphi},\varphi] = [\{\varphi_i\},\{\bar{\varphi}_i\}]$ represents sets of complex functions of imaginary time τ. In Eq. (25), $\beta = 1/k_B T$ with T being the temperature, $t_{ij} = t$ for nearest neighbors, and $t_{ij} = 0$ otherwise.

To explicitly explore the effects of hopping, characterized by t, on quantum fluctuations, we decouple the hopping term in Eq. (25) using the standard Hubbard-Stratonovich transformation [32]. By inserting a fat unity

$$\mathbf{1} = \int D[\bar{\Phi},\Phi] e^{-\frac{1}{\hbar}\int_0^{\hbar\beta} d\tau \sum_{\langle i,j\rangle} t_{ij} (\bar{\Phi}_i - \bar{\varphi}_i)(\Phi_j - \varphi_j)} \tag{26}$$

into Eq. (24), one transforms Eq. (24) to the phase space of new field variables $\{\bar{\Phi},\Phi\}$:

$$\begin{aligned} Z = \int D[\bar{\Phi},\Phi] \exp&\left(-\frac{1}{\hbar} \int_0^{\hbar\beta} d\tau \sum_{\langle i,j\rangle} t_{ij} \bar{\Phi}_i \Phi_j \right) \\ \times &\left\langle \exp\left(\frac{1}{\hbar} \int_0^{\hbar\beta} d\tau \sum_{\langle i,j\rangle} t_{ij} (\bar{\varphi}_i \Phi_j + \bar{\Phi}_i \varphi_j) \right) \right\rangle_0 . \end{aligned} \tag{27}$$

Here, $\langle \cdots \rangle_0 = \int D[\bar{\varphi},\varphi] \exp(-\frac{1}{\hbar} S^{(0)}[\bar{\varphi},\varphi])(\cdots)$ stands for the functional expectation value of an observable with

$$\begin{aligned} S^{(0)} = \int_0^{\hbar\beta} d\tau \Bigg[&\sum_i \bar{\varphi}_i \left(\hbar \frac{\partial}{\partial_\tau} - \mu\right) \varphi_i + \frac{U_0}{2} \sum_i \bar{\varphi}_i \bar{\varphi}_i \varphi_i \varphi_i \\ &+ \frac{U_d}{2} \sum_{\langle i,j\rangle} \bar{\varphi}_i \bar{\varphi}_j \varphi_j \varphi_i + \frac{W}{6} \sum_i \bar{\varphi}_i \bar{\varphi}_i \bar{\varphi}_i \varphi_i \varphi_i \varphi_i \Bigg] \end{aligned} \tag{28}$$

corresponding to $H^{(0)}$ in Eq. (12).

Information on excitations can be extracted from the grand-canonical partition function represented with new field variables $\{\bar{\Phi},\Phi\}$. To this end, we cast Eq. (27) into an effective expression

$$Z^{\text{eff}} = \int D[\bar{\Phi},\Phi] e^{-\frac{1}{\hbar} S^{\text{eff}}[\bar{\Phi},\Phi]}. \tag{29}$$

Here, the effective action $S^{\text{eff}}[\bar{\Phi},\Phi]$ can be determined from explicitly calculating the functional expectation term $\langle \cdots \rangle_0$ in Eq. (27). This can be achieved by first applying the Taylor expansion for exponential function $e^x = \sum x^n/n!$ and then carrying out the functional integration over the original field configuration $\{\bar{\varphi},\varphi\}$. Moreover, based on the fact that the site occupancy is fixed in the ground state of a MI phase [30], one has

$$\begin{aligned} \langle \varphi_i \rangle_0 &= \langle \bar{\varphi}_i \rangle_0 = 0, \\ \langle \bar{\varphi}_i \varphi_j \rangle_0 &= \langle \varphi_j \bar{\varphi}_i \rangle_0 = \langle \varphi_i \bar{\varphi}_i \rangle_0 \delta_{ij}. \end{aligned} \tag{30}$$

As a result, terms in odd powers of $\{\bar{\varphi},\varphi\}$ in the series of expansion must vanish. After some elaborated algebra, we obtain the effective action in Eq. (29) correct up to the second order in the hopping rate t as

$$\begin{aligned} S^{\text{eff}}[\bar{\Phi},\Phi] = &\int_0^{\hbar\beta} d\tau \sum_{\langle i,j\rangle} t_{ij} \bar{\Phi}_i \Phi_j - \frac{1}{\hbar} \int_0^{\hbar\beta} d\tau \int_0^{\hbar\beta} d\tau' \\ &\times \sum_{\langle i,jj'\rangle} \langle \bar{\varphi}_i(\tau) \varphi_i(\tau') \rangle_0 t_{ij} t_{ij'} \bar{\Phi}_{j'}(\tau') \Phi_j(\tau). \end{aligned} \tag{31}$$

To obtain the spectrum of the quasiparticle and quasihole excitations, however, it is more advantageous to transform Eq. (31) to the momentum-frequency space. The Fourier transformation of Eq. (31) reads

$$\begin{aligned} S^{\text{eff}}[\bar{\Phi},\Phi] = \sum_{n,k} |\Phi_{kn}|^2 \epsilon_k \Bigg\{ 1 + \epsilon_k \Bigg[&\frac{g}{E_g^{(0)} - E_{g-1}^{(0)} - i\hbar\omega_n} \\ &+ \frac{g+1}{E_g^{(0)} - E_{g+1}^{(0)} + i\hbar\omega_n} \Bigg] \Bigg\}, \end{aligned} \tag{32}$$

with $\Phi_i(\tau) = \frac{1}{\sqrt{N_s}} \sum_k e^{ikx_i} \Phi_k(\tau)$ and $\Phi_k(\tau) = \frac{1}{\sqrt{\hbar\beta}} \sum_n e^{-i\omega_n\tau} \Phi_{kn}$. Here, N_s is the number of lattice sites and the Matsubara frequencies are $\hbar\omega_n = 2n\pi/(\hbar\beta)$ with n being integers for bosons; $\epsilon_k = 2t \sum_{j=1}^d \cos(k_j a)$, and $E_g^{(0)} < \{E_n^{(0)}, n \neq g\}$ has the same form as Eq. (16) except without being scaled by zt. The quasiparticle (quasihole) spectra can then be obtained by replacing $i\omega_n \to \omega$ in Eq. (32) and scaling with zt as before. In a dimensionless form, one finds

$$\hbar\overline{\omega}_{\text{qp,qh}} = -\overline{\mu} + \frac{F(g) + F(g+1) - \bar{\epsilon}_k \pm \sqrt{\Delta_k}}{2}, \tag{33}$$

with

$$\Delta_k = [F(g+1) - F(g) - \bar{\epsilon}_k(2g+1)]^2 - 4\bar{\epsilon}_k^2 g(g+1) \tag{34}$$

and

$$\bar{\epsilon}_k = \frac{1}{d} \sum_{j=1}^d \cos(k_j a). \tag{35}$$

Here, the parameters with an overbar denote the dimensionless form for corresponding quantities after scaling. In Eq. (33), $\pm$ stands for excitations of quasiparticles (adding particles to sites) or quasiholes (removing particles from sites), respectively. The critical values for a transition from the superfluid to the Mott insulator are determined by requiring $\Delta_k \geqslant 0$:

$$\overline{U}_0 + z\overline{U}_d + \overline{W}(g-1) \geqslant [(2g+1) + \sqrt{4g(g+1)}]\bar{\epsilon}_k. \tag{36}$$

Let $\overline{U}_c$ and $\overline{W}_c$ denote the critical value of on-site two-body interaction $\overline{U}_0 + \overline{U}_d$ and three-body interaction $\overline{W}$, respectively. Equation (36) shows that both $\overline{U}_c$ and $\overline{W}_c$ exhibit dependence on the parameter g, but in different ways. Precisely, $\overline{U}_c$ increases with increasing g, whereas $\overline{W}_c$ decreases as $(g-1)^{-1}$ until asymptotically arriving at a fixed value $4\overline{\epsilon}_k$. In particular, $\overline{\epsilon}_k = 1$ for $k = 0$ and Eq. (36) approaches the phase boundary described by Eq. (23). Furthermore, for $g = 1$, $\overline{W}_c$ is divergent and $\overline{U}_c = 5.83$, while in the opposite case, $g \to \infty$, $\overline{W}_c = 4$, and $\overline{U}_c = 0$, all in good agreement with Ref. [24].

V. POSSIBLE EXPERIMENTAL SCENARIOS AND CONCLUSION

The work presented in this paper is based on an extended BHM that highlights the competition between kinetic energy and repulsive interactions that include both dipole-dipole and three-body interactions arising from triple collision. In particular, the physics of our model is characterized by the interplay among four parameters: the tunneling rate t, the two-body s-wave repulsion U_0, the dipole-dipole interaction U_d, and the three-body interaction W characterized by the three-body coupling constant. All these quantities are experimentally controllable using state-of-the-art technologies. First, tremendous progress has been achieved over the past few years in cooling and trapping polar molecules and atomic species that have a large magnetic moment [1]. This opened new windows in investigating degenerate gases with dominant dipole-dipole interactions. Second, the interatomic interaction can be controlled in a very versatile manner via the technology of Feshbach resonances [33], whereas the depth of an optical lattice s can be changed from $0E_R$ to $32E_R$ almost at will [2–5]. Third, there has been progress in identifying experimental accessible systems that exhibit three- and many-body interactions. In particular, Ref. [22] has pointed out that, by loading the polar molecules into the optical lattice and adding an external microwave field, one can achieve a situation where only observable three-body interaction among neighboring atoms exists. In addition for on-site interactions, Johnson [23] recently showed that there are effective three-body and higher interactions generated by the two-body collisions of atoms confined in the lowest vibrational states of a three-dimensional optical lattice. Consequently, for cold atoms loaded in an optical lattice, the ratio between the competing kinetic energy and the repulsive interactions can be readily changed by varying the dimensionless lattice depth V_0/E_R. The phenomena discussed in this paper, therefore, should be observable within the current experimental capability.

In summary, we investigated the quantum phases of a dipolar BEC in an optical lattice with both two- and three-body repulsive interactions. This was accomplished within the context of the extended BHM by using both the mean-field approach and the functional-integral approach. Accordingly, the phase diagrams from the superfluid state to the Mott-insulator state in such BEC systems were obtained. In particular, the combined effects of three-body and dipole-dipole interactions on the insulating *lobes* were explored in detail. The experimental scenario was also discussed.

ACKNOWLEDGMENTS

We thank Ying Hu for helpful discussions. This work is supported by the NSF of China (Grant No. 10674139). L.Z.X. is supported by an IMR SYNL-TS Ke Research Grant.

[1] T. Lahaye, C. Menotti, L. Santos, M. Lewenstein, and T. Pfau, Rep. Prog. Phys. **72**, 126401 (2009).
[2] I. Bloch, Nature Phys. **1**, 23 (2005).
[3] O. Morsch and M. Oberthaler, Rev. Mod. Phys. **78**, 179 (2006).
[4] I. Bloch, J. Dalibard, and W. Zwerger, Rev. Mod. Phys. **80**, 885 (2008).
[5] V. I. Yukalov, Laser Phys. **19**, 1 (2009).
[6] S. Ospelkaus, A. Pe'er, K. K. Ni, J. J. Zirbel, B. Nyenhuis, S. Kotochigova, P. S. Julienne, J. Ye, and D. S. Jin, Nature Phys. **4**, 622 (2008).
[7] K. K. Ni, S. Ospelkaus, M. H. G. de Miranda, A. Pe'er, B. Neyenhuis, J. J. Zirbel, S. Kotochigova, P. S. Julienne, D. S. Jin, and J. Ye, Science **322**, 231 (2008).
[8] J. Deiglmayr, A. Grochola, M. Repp, K. Mörtlbauer, C. Glück, J. Lange, O. Dulieu, R. Wester, and M. Weidemüller, Phys. Rev. Lett. **101**, 133004 (2008).
[9] A. Griesmaier, J. Werner, S. Hensler, J. Stuhler, and T. Pfau, Phys. Rev. Lett. **94**, 160401 (2005).
[10] C. Menotti, M. Lewenstein, T. Lahaye, and T. Pfau, in *Dynamics and Thermodynamics of Systems with Long-Range Interaction: Theory and Experiments*, AIP Conf. Proc. No. 970, edited by A. Campa, A. Giansanti, G. Morigi, and F. Sylos Labini (AIP, New York, 2008).
[11] S. Yi and L. You, Phys. Rev. A **61**, 041604(R) (2000); **63**, 053607 (2001).
[12] K. Góral, K. Rzazewski, and T. Pfau, Phys. Rev. A **61**, 051601(R) (2000); J. P. Martikainen, M. Mackie, and K. A. Suominen, *ibid.* **64**, 037601 (2001); K. Góral and L. Santos, *ibid.* **66**, 023613 (2002).
[13] L. Santos, G. V. Shlyapnikov, P. Zoller, and M. Lewenstein, Phys. Rev. Lett. **85**, 1791 (2000).
[14] H. Pu, W. P. Zhang, and P. Meystre, Phys. Rev. Lett. **87**, 140405 (2001); W. Zhang, H. Pu, C. Search, and P. Meystre, *ibid.* **88**, 060401 (2002).
[15] S. Giovanazzi, D. O'Dell, and G. Kurizki, Phys. Rev. Lett. **88**, 130402 (2002).
[16] B. Capogrosso-Sansone, S. Wessel, H. P. Büchler, P. Zoller, and G. Pupillo, Phys. Rev. B **79**, 020503(R) (2009).
[17] D. Jaksch, J. I. Cirac, P. Zoller, S. L. Rolston, R. Cote, and M. D. Lukin, Phys. Rev. Lett. **85**, 2208 (2000).
[18] G. K. Brennen, C. M. Caves, P. S. Jessen, and I. H. Deutsch, Phys. Rev. Lett. **82**, 1060 (1999); G. K. Brennen, I. H. Deutsch, and C. J. Williams, Phys. Rev. A **65**, 022313 (2002); D. DeMille, Phys. Rev. Lett. **88**, 067901 (2002).
[19] T. T. Wu, Phys. Rev. **115**, 1390 (1959).
[20] E. Braaten and A. Nieto, Eur. Phys. J. B **11**, 143 (1999); E. Braaten, H.-W. Hammer, and S. Hermans, Phys. Rev. A **63**, 063609 (2001).

[21] T. Köhler, Phys. Rev. Lett. **89**, 210404 (2002).

[22] H. P. Büchler, A. Micheli, and P. Zoller, Nature Phys. **3**, 726 (2007).

[23] P. R. Johnson, E. Tiesinga, J. V. Porto, and C. J. Williams, New J. Phys. **11**, 093022 (2009).

[24] B. L. Chen, X. B. Huang, S. P. Kou, and Y. B. Zhang, Phys. Rev. A **78**, 043603 (2008).

[25] E. A. Efimov, Phys. Lett. B **33**, 563 (1970).

[26] E. Braaten, H. W. Hammer, and T. Mehen, Phys. Rev. Lett. **88**, 040401 (2002); A. Bulgac, *ibid.* **89**, 050402 (2002).

[27] C. J. Pethick and H. Smith, *Bose-Einstein Condensation in Dilute Gases* (Cambridge University Press, Cambridge, England, 2002).

[28] C. Menotti, C. Trefzger, and M. Lewenstein, Phys. Rev. Lett. **98**, 235301 (2007).

[29] T. Lahaye, T. Koch, B. Fröhlich, M. Fattori, J. Metz, A. Griesmaier, S. Giovanazzi, and T. Pfau, Nature (London) **448**, 672 (2007).

[30] D. van Oosten, P. van der Straten, and H. T. C. Stoof, Phys. Rev. A **63**, 053601 (2001).

[31] A. Messiah, *Quantum Mechanics* (North-Holland, Amsterdam, 1961), Vol. 2.

[32] A. Altland and B. Simons, *Condensed Matter Field Theory* (Cambridge University Press, Cambridge, England, 2006).

[33] E. Tiesinga, B. J. Verhaar, and H. T. C. Stoof, Phys. Rev. A **47**, 4114 (1993); S. Inouye *et al.*, Nature (London) **392**, 151 (1998).